Theoretical and Applied Climatology (2020) 141:525–536
https://doi.org/10.1007/s00704-020-03188-2

ORIGINAL PAPER

Evaluation of NASA's NEX-GDDP-simulated summer monsoon rainfall over homogeneous monsoon regions of India

Praveen Kumar[1] · Sunny Kumar[1] · Archisman Barat[1] · P. Parth Sarthi[1] · Ashutosh K. Sinha[1]

Received: 24 May 2019 / Accepted: 19 March 2020 / Published online: 5 May 2020

Abstract

The current research aimed to evaluate the predictive skill of statistically downscaled National Aeronautics Space Administration (NASA) Earth Exchange Global Daily Downscaled Projection (NEX-GDDP) data in simulating the Indian summer monsoon rainfall (ISMR) for the period of 1961–2005 over the individual homogeneous monsoon regions of India (HMRI). For the purpose, five models are selected, as these models (in GCM) have shown better performance in the simulation of ISMR by the researcher. The spatial characteristics and statistical scores (annual cycle, percentage bias, Taylor score, probability distribution function) are used to evaluate the performance of each model in simulating rainfall over land points of individual HMRI. In the spatial analysis, it seems that models of NEX-GDDP can simulate the ISMR, pretty well in comparison to APHRODITE (observation), and show a moderate to significantly high correlation (grid point) over each of the HMRI particularly to core monsoon region, except over few parts of PI. The Taylor statistics suggest that the model CanESM performs very well over the regions of PI, NWI, and WCI. The models MPI-ESM-LR and NorESM perform well in simulating the ISMR over CNI, followed by ACCESS, CanESM, and CCSM4. The models have varying bias in predicting the rainfall; however, ACCESS does perform well and shows the minimum bias (ranges from ~ 1 to ~ 14% only) among others. The models CanESM and NorESM (except over CNI) performed relatively better. The NEX-GDDP models overcome the global climate models (GCMs) in the retrospective simulation of ISMR over the land points of India. It is concluded that the models have good predictability of JJAS rainfall but unable to catch daily rainfall variability.

1 Introduction

The summer monsoon rainfall is an essential parameter for agricultural production, water supply, and livelihood in India. However, relatively accurate quantification of summer monsoon rainfall for future periods at the regional and local scale is a challenging task owing to its erratic behavior and skewed statistics (Meher et al. 2017). The varying orography and land-sea contrast make the uneven distribution of rainfall over landmasses of India, and therefore, the predictability of rainfall is always a challenging task. Global climate models (GCMs) are used to predict the rainfall but unable to provide information on regional/smaller scales (Solomon et al. 2007). To improve prediction, in the 1990s, World Climate Research Programme (WCRP) coordinated Coupled Model Intercomparison Project (CMIP) has been carried out on control experiment and variety of sensitivity experiments (Meehl et al.2000), and further additional phases of the CMIP, termed as CMIP2, CMIP2+, CMIP3, CMIP5, and recently CMIP6, have been performed. There are numerous studies on validation and future projection of rainfall in CMIP3 and CMIP5 model experiments over the land points of India (Sarthi et al. 2015, 2016); however, projection of summer monsoon rainfall under changing climate using GCMs is still challenging for the researchers (Pattnaik and Kumar 2010; Turner and Annamalai 2012). In addition to that, uncertainties are associated with GCMs in the prediction of monsoon rainfall due to the vastness of GCMs, coarse resolution, and not proper inclusion of local or regional factors (Christensen et al. 2008; Saini et al. 2015).

To provide information on regional scales for agricultural planning, water resources management, power industry, and environmental policymaking, the prediction of rainfall through coarse resolution GCMs is not sufficient (Maraun et al. 2010). In general, the globally available GCMs outputs at coarser resolution (varying resolution of 1.0–2.5°) (Pepler

✉ P. Parth Sarthi
drpps@hotmail.com

[1] Department of Environmental Science, Central University of South Bihar, Gaya, Bihar 824236, India

et al. 2016) are mandatory to be scaled down to local scales and are done by either dynamical or statistical downscaling. To provide the information at a regional scale, there are varieties of dynamical downscaling and statistical downscaling techniques developed in the last decades (Wilby and Wigley 1998; Mearns et al. 1999; Maraun et al. 2010; Sunyer et al. 2012; Ekström et al. 2015). The statistical technique uses empirical relation between large-scale climate predictors from GCMs and the local scale predictants of real-time observation (station data) of interest (Huang et al. 2011; Wilby et al. 1998). The dynamical downscaling technique employs regional climate models (RCM) using the output of GCMs (Fowler et al. 2007, Giorgi 1990). On the end, the widely used statistical downscaling is more applicable than dynamical downscaling (Sun and Chen 2012), because of its easy implementation, low computation effort (Fowler et al. 2007), and ability to provide point scale outputs (Wilby et al. 2002). However, there is no best suited downscaling approach since all these approaches depend on the desired spatial and temporal resolution of outputs and the climate characteristics of the region of interest (Trzaska and Schnarr 2014). The statistical downscaling methods such as the WEather GEnerator (WGEN), the Long Ashton Research Station-Weather Generator (LARS-WG), and the Statistical Downscaling Model (SDSM) (Hashmi et al. 2011; Mahmood and Babel, 2013) are recently developed.

To fulfill the requirements and necessity of downscaled climate data, NASA applied statistical downscaling techniques on GCMs of the CMIP5, to generate a high-resolution dataset for long-term projections, called "NASA Earth Exchange Global Daily Downscaled Projections" (NEX-GDDP), which have been released on June 2015 (Thrasher et al. 2013). Raghavan et al. (2018) have used NEX-GDDP data for examining NEX-GDDP dataset over Southeast Asia in historical (1976–2005) and future (2020–2050, 2070–2099) periods (under RCP 4.5 and 8.5), for rainfall and surface temperature at a surface resolution of 25 km on a daily basis. Over China, the NEX-GDDP data has been evaluated for their performance in simulating the extremes of rainfall and climate changes (Chen et al. 2017). The historical dataset shows good agreement with observations on monthly scales but fails to capture daily statistics. Sahany et al. (2019) validated the NEX-GDDP and NCAR-CCSM4 model under CMIP5 experiments and suggested an underestimation of rainfall extremes by CCSM4-CMIP5 than the CCSM4-NEX-GDDP. Both CCSM4-CMIP5 and CCSM4-NEX-GDDP have projected an increase in annual rainfall over India, under the RCP8.5. Worth noting is that the extreme daily rainfall values projected by CCSM4-NEX-GDDP are two to three times larger than that projected by CCSM4-CMIP5.

As mentioned earlier, the simulation (in the past and future periods) of June-July-August-September (JJAS) rainfall over monsoon homogeneous regions is still a challenging task due to different physics and parameterization schemes applied in the models (Christensen and Christen, 2007). To fulfill this gap, the newly available NEX-GDDP rainfall data (https://nex.nasa.gov/nex/projects/1356) provided by NASA in multiple climate models are evaluated for JJAS rainfall over India. The current study may be a novel approach for the assessment of NEX-GDDP in capturing the characteristics of observed rainfall over individual HMRI.

In this paper, the first section discusses the existing literature over the pros and cons of the spatial resolution of GCMs and dynamically downscaled RCMs in simulation and statistical downscaling of ISMR and, in last, describes the major objective of current research. Section 2 consists of data and methods, followed by Sect. 3 that discusses the result and discussion. The conclusions are placed in Sect. 4.

2 Study area, data, and methods

2.1 Study area

In this study, the five homogeneous monsoon regions of India are considered (Parthasarathy et al. 1993). The five homogeneous region are (i) North West India (NWI), (ii) West Central India (WCI), (iii) Central Northeast India (CNI), (iv) North East India (NEI), and (v) Peninsular India (PI), as shown in Fig. 1 (Source: IITM, Pune, India), and there are regional differences in the monsoon rainfall variability over each homogeneous monsoon region (Parthasarathy 1984; Walker 1925; Shukla 1987, Gregory 1989). In the present study, the Himalayan Region (HR) of India is not included due to fewer numbers of observations and is also distantly located (Rajeevan et al. 2006). The well-validated NASA's NEX-GDDP models data at finer resolution may be helpful for impact assessment to sectors like hydrology, agriculture, economics, and others, in the near and far future period.

2.2 Data

The high-resolution daily rainfall data of NASA Earth Exchange Global Daily Downscaled Projection (NEX-GDDP) at surface resolution 0.25° (~ 25 km × 25 km) is the output of twenty-one (21) GCMs of CMIP5 and is available for the period of 1950–2100 (during 1950–2005, in hindcast/retrospective run, and 2006–2099 in prospective run). Since these data provide climate change information in the past and future periods at the finest possible scales (Thrasher et al. 2012a, b), therefore, the dataset may be used for climate change assessment study at a city/basin level. The details of the methodology applied in generating this data are explained by Maurer and Hidalgo (2008), Thrasher et al. (2012a, b), Thrasher et al. (2013), and Wood et al. (2004). The bias correction spatial disaggregation (BCSD) method is used to

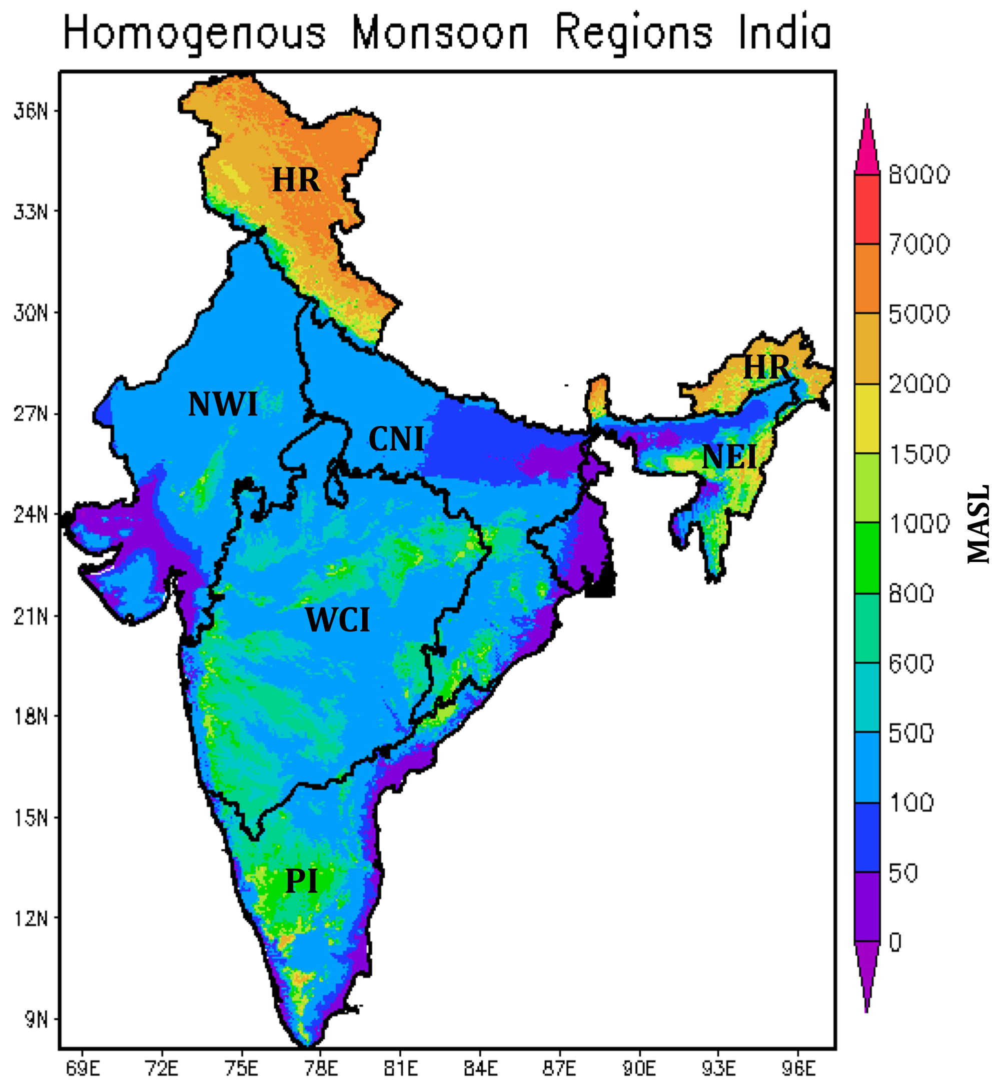

Fig. 1 General overview of terrain in homogeneous monsoon region of India (HMRI). (Dem Data source: http://clima-dods.ictp.it/data/Data/RegCM_Data/SURFACE/)

produce the NEX-GDDP datasets. The BCSD is a statistical downscaling algorithm that addresses limitations of global GCM outputs (coarser resolution and biased at regional/local scale) (Wood et al. 2002, 2004; Thrasher et al. 2012a, b). For the purpose, five models, namely, ACCESS, CanESM, CCSM4, MPI-ESM-LR, and NorESM of NEX-GDDP, are considered and shown in Table 1. These five models (under CMIP5 experiment) have shown better performance in the simulation of JJAS rainfall (Sarthi et al. 2015, 2016; McSweeney et al. 2015; Sonali et al. 2017). The NEX-GDDP data of these selected GCMs are

Table 1 List of NASA NEX-GDDP datasets included from CMIP5 models

Model	Spatial Resolution
ACCESS1-0	0.25°× 0.25°
CanESM2	0.25°× 0.25°
CCSM4	0.25°× 0.25°
MPI-ESM-LR	0.25°× 0.25°
NorESM1-M	0.25°× 0.25°

taken from the NASA data portal (ftp://ftp.nccs.nasa.gov/ NEX-GDDP). The observational data (either station data or grid data) plays an important role as reference value for the model's evaluation, and therefore, the gridded data from the experiment of Asian Precipitation-Highly Resolved Observational Data Integration Towards Evaluation (APHRODITE) at a spatial surface resolution of 0.25° (~25 km × 25 km) is considered (Yatagai et al. 2012) for the period of 1961–2005.

2.3 Methodology

To find the correlation, at each grid between rainfall in observations and each of five selected model simulation rainfall, grid point correlation (GPC) is calculated at each of the grid points over regions of HMRI, as shown in Fig. 2.The annual and seasonal (JJAS) rainfall data is area averaged over the land point for individual HMRI, and is considered for the period of 1961-2005. The annual and seasonal (JJAS) rainfall is area-averaged over land points of individual HMRI for the

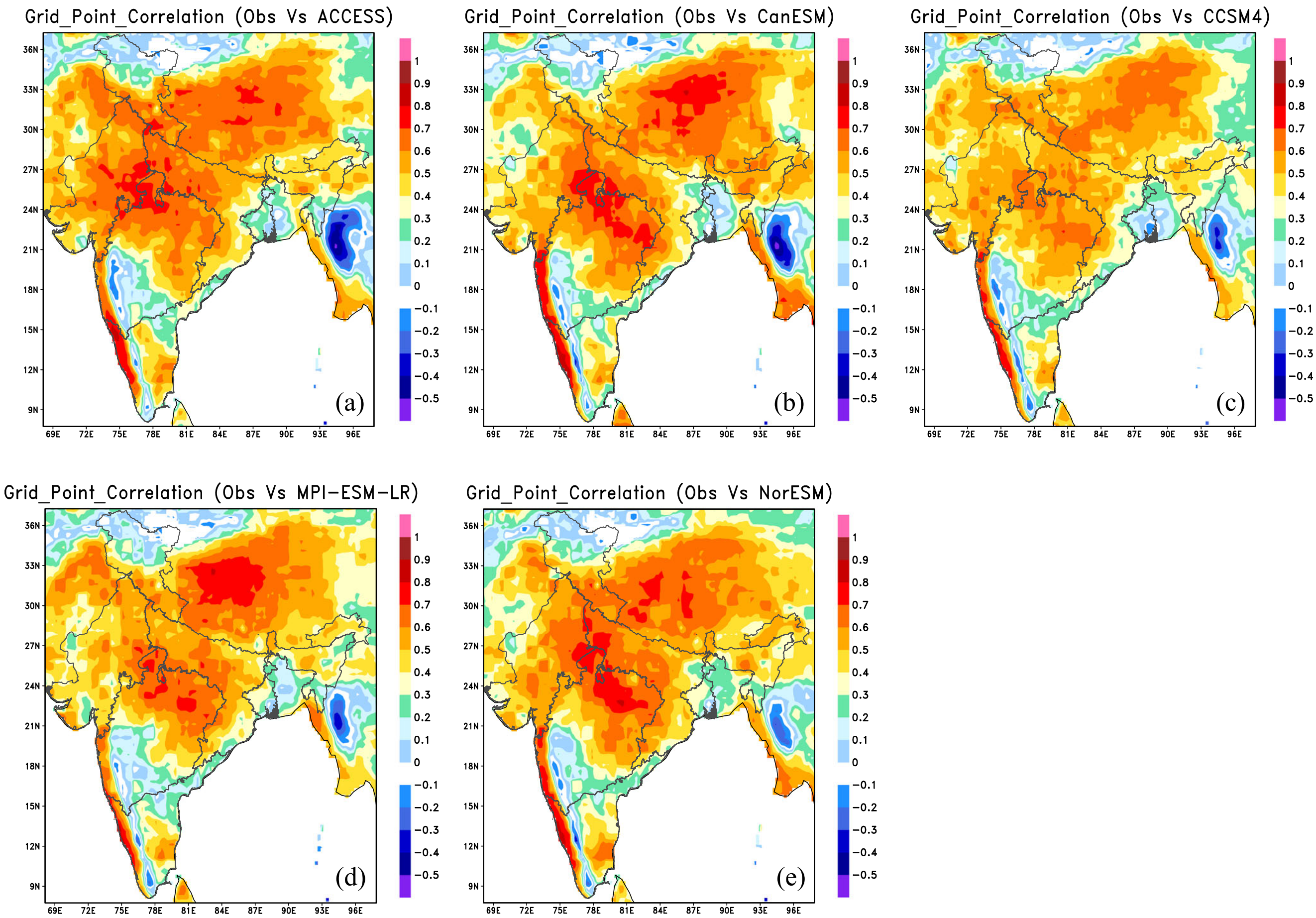

Fig. 2 Grid point correlation (GPC) between observation and (**a**) ACCESS, (**b**) CanESM, (**c**) CCSM4, (**d**) MPI-ESM-LR, and (**e**) NorESM

period of 1961–2005. Further, the models' ability for simulating the ISMR for the past time period, over individual HMRI, is assessed by comparing the daily climatology, distribution of rainfall using box plot, the probability density function (PDF), the Taylor (2001) statistics, and percentage bias. For the spatial distribution, mean JJAS rainfall is considered for a retrospective run (1961–2005).

3 Results and discussion

3.1 Spatial distribution of ISMR over HMRI

The GPC between observations and simulated rainfall at each grid points over different regions is carried out by many researchers (Guhathakurta and Rajeevan, 2008; Sagar et al., 2017; Mandal et al., 2006). The GPC of JJAS rainfall between the model of NEX-GDDP and observation is shown in Fig. 2a–e. The GPC, which varies from 0 (no correlation) to 1 (strong correlation), is presented for individual HMRI. A strong positive GPC between observation and simulated JJAS rainfall of ACCESS, CanESM, CCSM4, MPI-ESM-LR, and NorESM is noticed over WCI and parts of NWI and CNI, which are the core monsoon regions of India (Sinha et al. 2007). The western part of WCI and PI also shows a strong GPC. The other regions have relatively weaker GPC. It seems that NEX-GDDP models simulated JJAS rainfall shows strong GPC over core monsoon regions of India. It might be attributed to better representation of orography in the driving model (GCMs here), leading to well capturing of the JJAS rainfall pattern over the regions (core monsoon region of India). The orography represented in GCMs, as well as appropriate parameterizations and convection schemes, may make it possible to cover the large-scale monsoon dynamics here (Xie et al. 2006). It may be emphasized that the best model for a particular area may not necessarily be the best performer over other regions (Errasti et al. 2011).

3.2 Temporal variability of ISMR over HMRI

In Fig. 3a–e, the daily JJAS rainfall climatology is shown in observation and simulation for the period of 1961–2005 over CNI, WCI, NWI, PI, and NEI. It seems that the NEX-GDDP-simulated daily JJAS rainfall is following the observed pattern, with varying magnitude (in the range of −3 to 3 mm/day), of rainfall over each HMRI. Over CNI (Fig. 3a), the

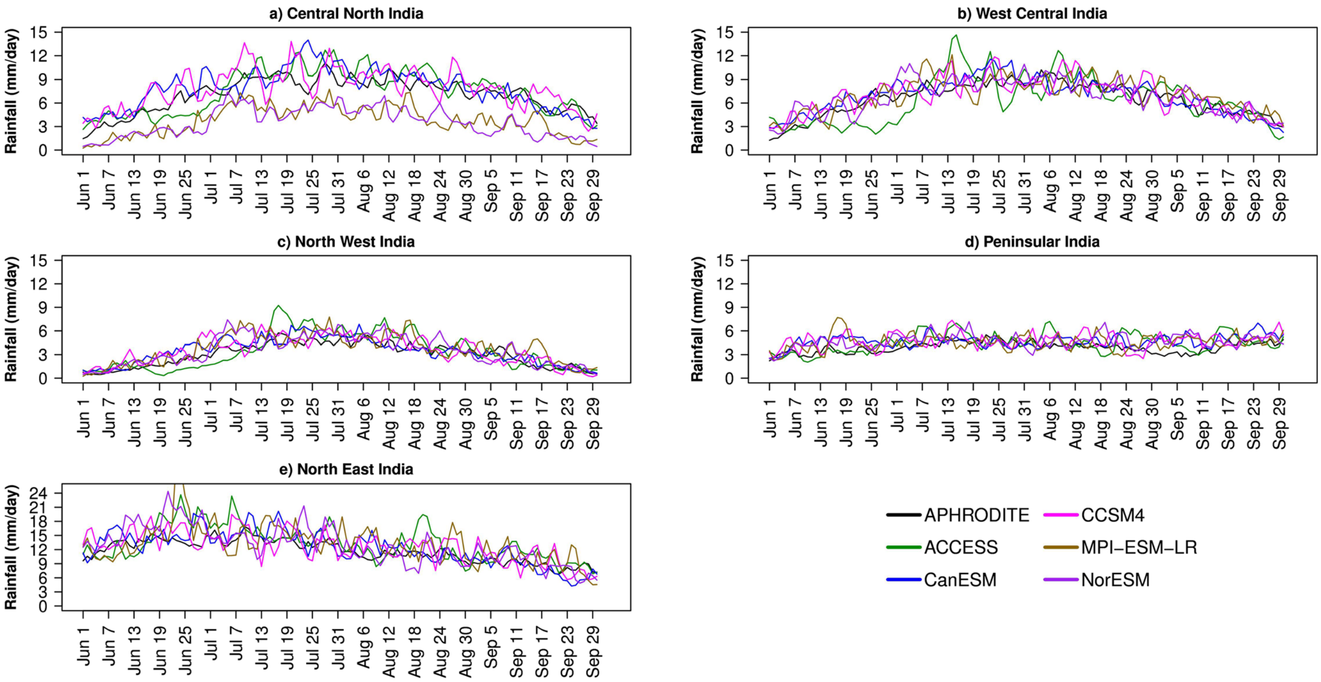

Fig. 3 Daily climatology during June1–September 30 in NEX-GDDP-simulated and observed rainfall (APHRODITE) over CNI (**a**), WCI (**b**), NWI (**c**), PI (**d**), and NEI (**e**)

simulated rainfall shows a considerable large variation with observations; however MPI-ESM-LR- and NorESM-simulated rainfall show underestimation in comparison to the observation. Here, large variation means the degree to which rainfall amounts vary through time from the mean (not including the extremes). Further, the ACCESS-simulated rainfall shows large-scale variation compared with observation over regions of CNI, WCI, NWI, and NEI. In similar ways, Raghavan et al. (2018) suggest that over South Asia, NEX-GDDP-simulated daily rainfall statistics are not close to observation. Over the UK, Rivington et al. (2008) found that RCM-simulated rainfall during 1960–1990 shows an excess of small (< 0.3 mm) precipitation events in observation while overestimating the annual mean and underestimating at different places. It seems that the effect of topography in model simulations occasionally excites or intensifies precipitation extremes. Therefore high-resolution NEX-GDDP dataset (Bao and Wen, 2017) may not follow the extremes in observation.

The time series analysis is carried out to characterize the trend in JJAS-accumulated rainfall for the period of 1961–2005 over individual HMRI as shown in Fig. 4a–e. Over the region of CNI (Fig. 4a), all models perform relatively well in capturing trend of JJAS rainfall except ACCESS (overestimation). However, during the period of 1975–1995, a small bias is observed by the model. Over WCI, the models ACCESS and CCSM4 show significant positive and negative bias, while other models show an excellent predictability of JJAS rainfall. The models CCSM4, NorESM, CanESM, and MPI-ESM-LR follow the observed trend over the Penisular India. Over NEI, all the models show significant variability in comparison to observation. Again, over the region, NEI, CanESM, and CCSM4 outperform the trend. Further, an overview of the annual cycle is analyzed to determine how well each model does follow the pattern of the observed annual cycle. The annual cycle of simulated rainfall for the period of 1961–2005 is constructed for the initial evaluation of the model's performance (Sarthi et al., 2015) and shown in Fig. 5a–e. The annual climatology is obtained by averaging the monthly data over the period of 1961–2005. The result shows that NEX-GDDP rainfall, except in a few cases (models), follows the pattern of observations. Over the CNI, CanESM-simulated rainfall is an overestimation of observation; however, over the PI, all models are overestimating (with less bias) in comparison to observations for the rainy months of August and September (highest). During the initial monsoon month (June), the models are overestimating (with less bias) over the region NEI. Over the region of NWI, the models are overestimating (slightly) during the month of July, while it shows a good resemblance with observation for all months. All models are showing resemblance with the observed pattern during the monsoon months.

To evaluate model's performance in terms of the shape of the distribution, its central value, and its variability, the box and whisker plots are used (Sarthi et al. 2015, 2016; Rana et al. 2012; Durai and Bhardwaj, 2014; Saha et al. 2014; Ghosh et al. 2016). Figure 6 a and e show box plots of observed and simulated JJAS rainfall for CNI, WCI, NWI, PI, and NEI. The median of simulated JJAS rainfall shows good agreement with observation over WCI (Fig. 6b), NWI

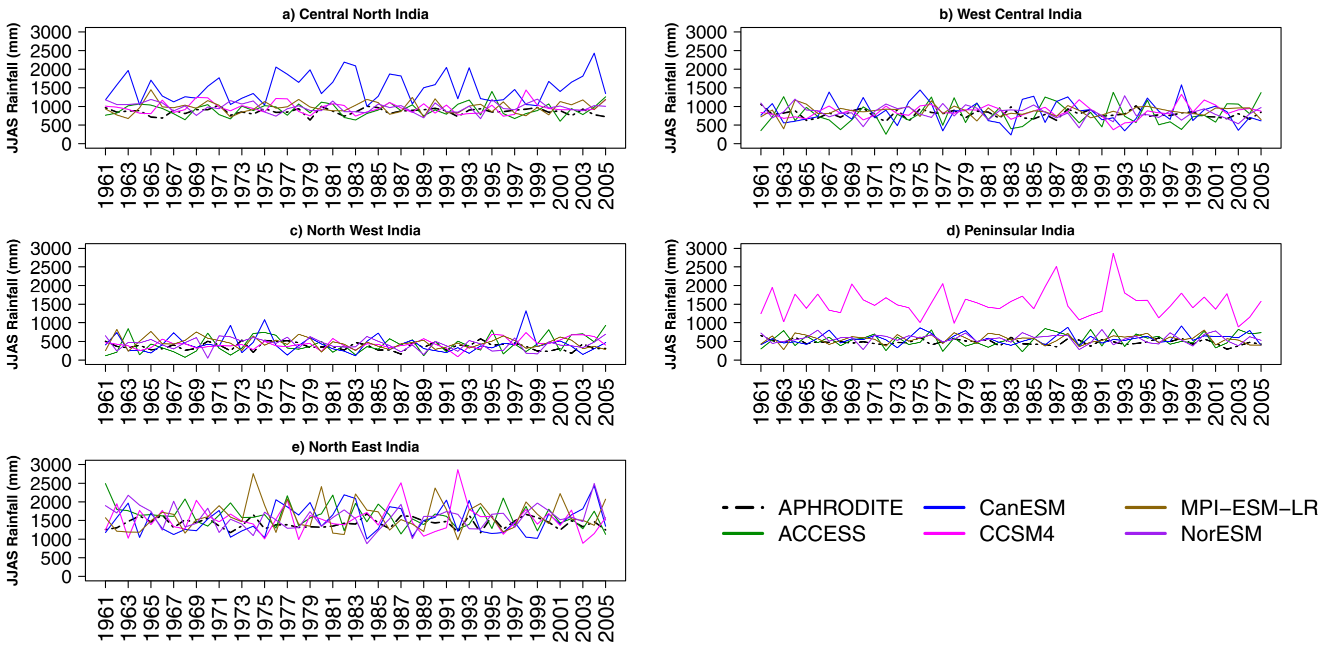

Fig. 4 Trend of JJAS rainfall over HMRI, in observation (APHRODITE) and datasets of NEX-GDDP

(Fig. 6c), PI (Fig. 6d), and NEI (Fig. 6e), whereas models MPI-ESM-LR- and NorESM-simulated median of JJAS rainfall are not close to observation over CNI. It seems that over the regions of large rainfall variability like CNI and WCI, the NEX-GDDP-simulated rainfall is not relatively closer to observations, while regions of small variability of rainfall like NWI, PI, and NEI in NEX-GDDP show good agreement in median as well as in the range (maximum and minimum values) of observed rainfall.

Based on relatively low standard deviation (SD), high correlation, and low root mean square error (RMSE) of model's simulated by JJAS rainfall in comparison to observations, the Taylor analysis is carried over individual HMRI as shown in Fig. 7a–e. In the Taylor plot, Pearson's correlation is shown along the circular axis, and a strong value is located close to observation on the x-axis. The normalized standard deviation (SD) of observation is taken as one, and the same is shown in terms of its distance from the observation. Similarly, root mean square error (RMSD) of each model is shown as the

Fig. 5 Annual cycle for NEX-GDDP models and observations over CNI (**a**), WCI (**b**), NWI (**c**), PI (**d**), and NEI (**e**)

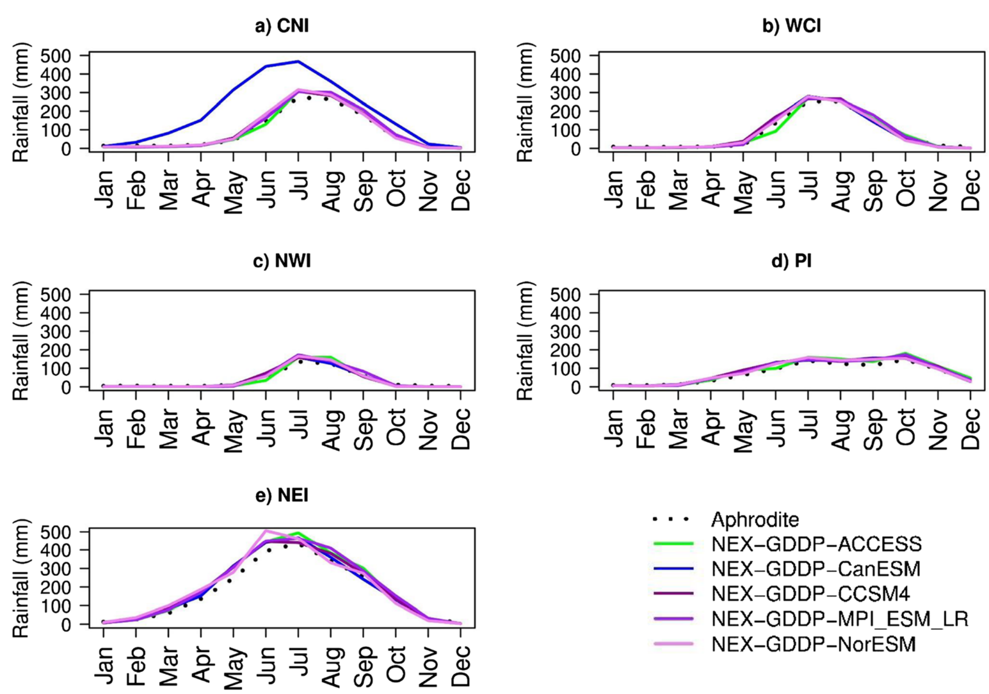

distance from the observations on the x-axis (Taylor et al. 2012). The radial distance from the observation shows the actual performance of each model, the closer (radially) from observation, the more accurate in predicting the ISMR over particular HMRI. All models have different capabilities to simulate the ISMR compared to observation; hence, the Taylor score for each of the models varies. It is noticed that the NEX-GDDP-CanESM is performing relatively better than other downscaled models over NEI, PI, NWI, and WC, while NEX-GDP-MPI_ESM_LR is performing relatively better than others over CNI. The model MPI-ESM-LR and NorESM do well in simulating the ISMR over CNI and followed by ACCESS, CanESM, and CCSM4. Similarly, the model CanESM performs very well over the regions of PI, NWI, and WCI. It seems that the relative performance of downscaled NEX-GDDP models varies over individual HMRI (Sahany et al. 2019; Raghavan et al. 2018).

The percentage bias (PBIAS) is another way to assess NEX-GDDP model performance. Table 2 shows the different statistical scores for considered models (compare to observations) of NEX-GDDP over each of the HMRI. The result shows the positive PBIAS over PI of HMRI; however, the highest PBIAS is predicted by the model CCSM4 and lowest with ACCESS model. The CNI region of HMRI has large negative PBIAS in the simulation of NorESM (− 50.5) and MPI-ESM-LR (− 47.2), while a small positive PBIAS is predicted by ACCESS (5.4), CanESM (10.9), and CCSM4 (11.3) simulations. The PBIAS is highest over the region of NWI in MPI-ESM-LR, while over WCI region, a negative (but small) PBIAS is predicted by ACCESS model. It is very interesting that all models can simulate the JJAS rainfall with good confidence, except over PI in the high-resolution NEX-GDDP dataset (Bao and Wen, 2017).

Examining climate statistics other than climate means is not new, and, earlier, researchers have used probability distribution functions (PDF) to analyze the frequency and severity of climate extremes. The PDF is used to understand model's ability in simulating rainfall on daily basis during monsoon season, while monthly rainfall analysis is carried out to see how models are simulating monthly rainfall. Researchers have already reported that many climate models fail to simulate

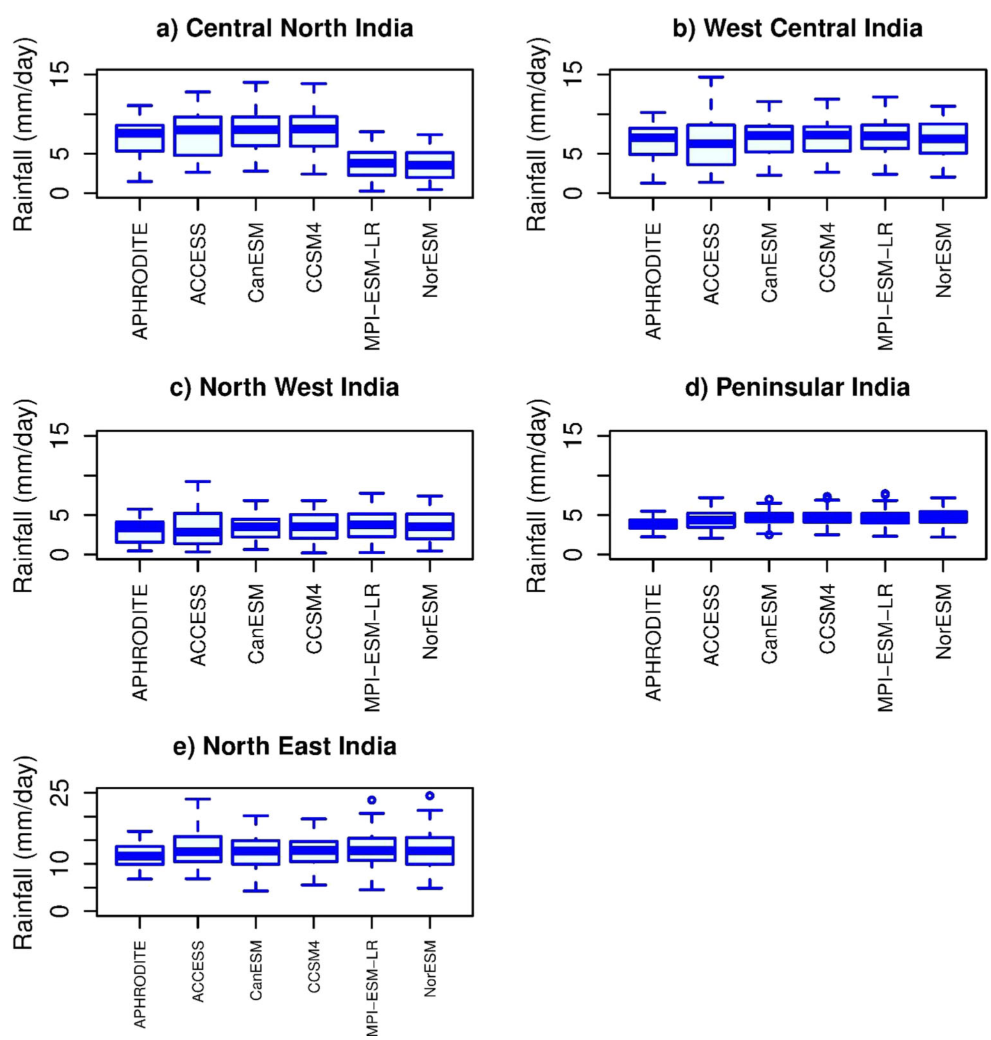

Fig. 6 Box plots for NEX-GDDP-simulated and observed JJAS rainfall over CNI (**a**), CI (**b**), NWI (**c**), PI (**d**), and NEI (**e**)

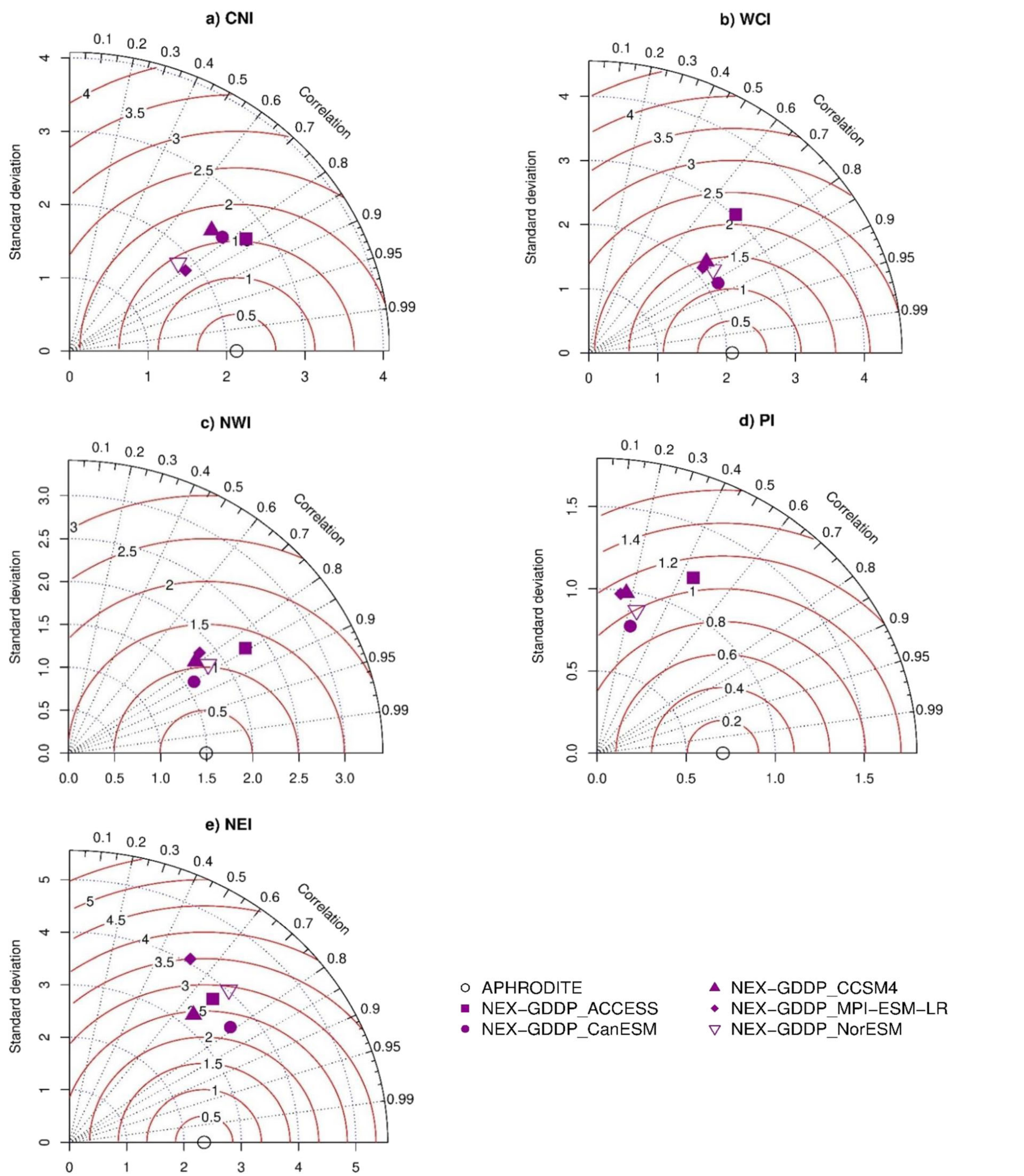

Fig. 7 Taylor's diagram for JJAS rainfall in NEX-GDDP-simulated and observed rainfall (APHRODITE) over CNI (**a**), WCI (**b**), NWI (**c**), PI (d), and NEI (**e**)

rainfall on a daily/monthly basis although they reasonably well simulate seasonal rainfall. To investigate the possible shifts in daily rainfall probability (Bokhari et al. 2018), the PDF on daily rainfall (during 1961–2005) in observation and model simulation over each of HMRI is shown in Fig. 8a–e. Over CNI, the frequency of daily rainfall in the simulation of NEX-GDDP-CanESM and NEX-GDDP-CCSM4 shows good agreement with observation and found to be in the range of 01–09 mm day^{-1}. The model NEX-GDDP-ACCESS-simulated rainfall shows good agreement with the ranges of observed rainfall of 1–4 mm day^{-1}. Other models, NEX-GDDP-MPI-ESM-LR and NEX-GDDP-NorESM, have underestimated the daily observed rainfall frequency. The models CanESM, CCSM4, and ACCESS show good agreement with a daily range of rainfall between 11 and 15 mm day^{-1}. Over the NEI of India, each model shows good agreement with the frequency of rainfall in the range of 1–8 mm day^{-1}. However, the overestimation and underestimation

Table 2 Percentage bias (PBIAS) prediction by model over individual HMRI

	CNI	WCI	NWI	PI	NEI
ACCESS	5.4	− 1.2	12.1	13.8	13.9
CanESM	10.9	6.0	13.9	19.1	6.1
CCSM4	11.3	7.7	17.3	20.2	8.0
NorESM	− 50.5	5.3	16.6	19.6	10.6
MPI-ESM-LR	− 47.2	9.1	24.6	16.3	13.1

are very low in frequency, and it is suggested that all models are performing well in a rainfall probability distribution. While considering the performance of models over NWI, all five models have similar rainfall probability in daily rainfall of 1–3 mm day^{-1}. The NEX-GDDP-CCSM4 does follow the frequency of daily climatological rainfall over the entire range of observed rainfall. However, overestimation in frequency is found for the remaining four models. Compare to observation, the models (NorESM and CCSM4) show underestimate (very slight in magnitude) of the rainfall frequency in the range of 4–5 mm day^{-1}, but highly underestimation in frequency in the range of 3–7 mm day^{-1}. Over the WCI, except ACCESS and NorESM, all models do perform quite well in the entire range of rainfall, but ACCESS and NorESM models do underestimate the entire frequency range of daily rainfall. It is further observed that over PI, the frequency of daily rainfall is more in all models as compared with other regions of HMRI and underestimates the rainfall frequency; however, in the range of 2–4 mm day^{-1}, all model performs well in predicting the daily frequency.

It is generally accepted that the model that performed better in the current climate is considered as the model with a more reliable future projection (Errasti et al. 2011; Zamani and Berndtsson, 2018). It may be suggested that the model shows

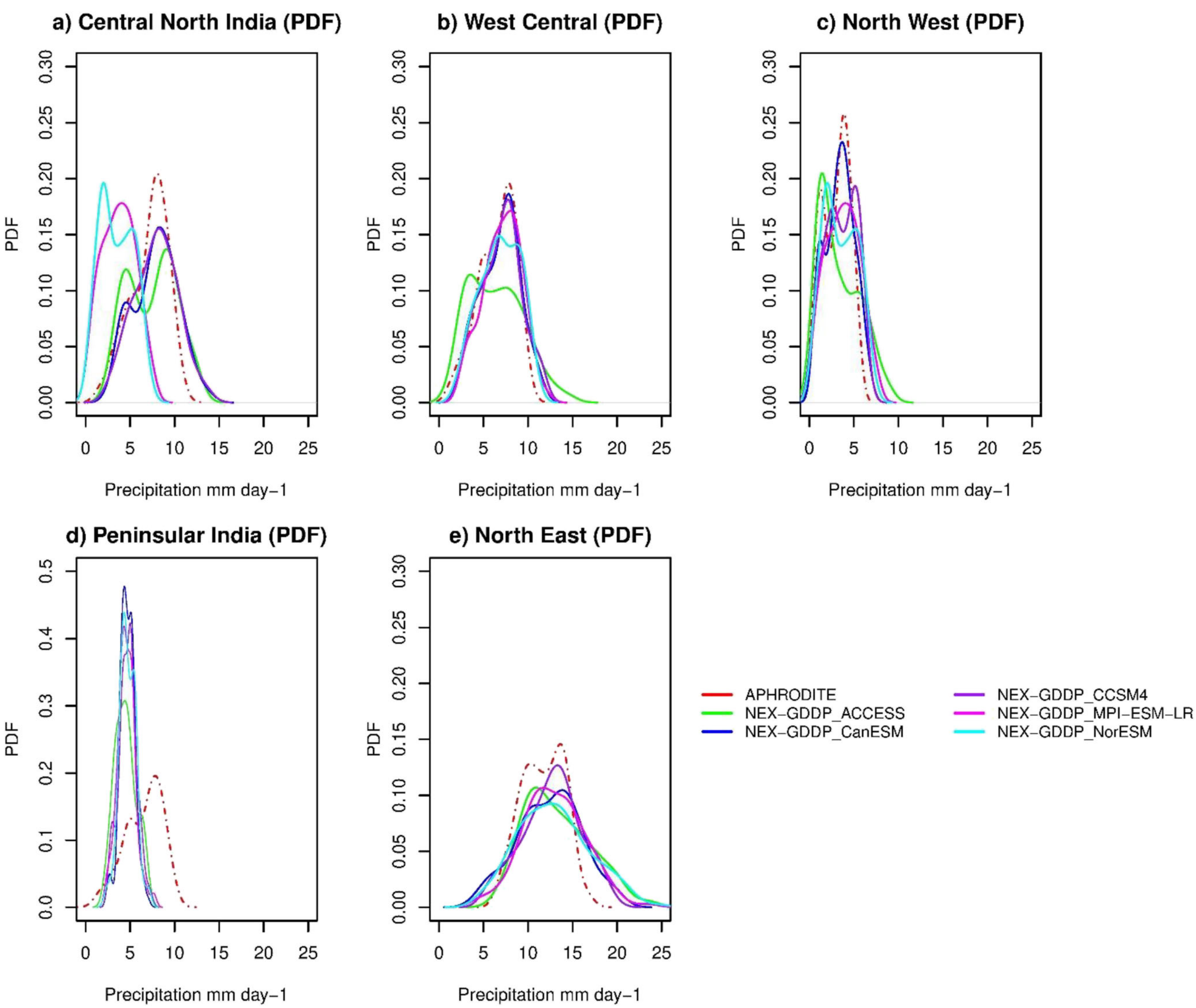

Fig. 8 Probability distribution function for NEX-GDDP models and observations over CNI (**a**), WCI (**b**), NWI (**c**), PI (**d**), and NEI (**e**)

Table 3 Relative performance of model in predicting the JJAS rainfall over HMRI

Central North India	West Central India	North West India	Peninsular India	North East India
MPI-ESM-LR	CanESM	CanESM	CanESM	CanESM
NorESM	NorESM	NorESM	NorESM	CCSM4
ACCESS	MPI-ESM-LR	CCSM4	ACCESS	ACCESS
CanESM	CCSM4	MPI-ESM-LR	MPI-ESM-LR	NorESM
CCSM4	ACCESS	ACCESS	CCSM4	MPI-ESM-LR

good skill, against observation, in simulating rainfall in historical experiment which may be (probabilistically) a good predictor for the future time period (Reichler and Kim 2008). Hence, the selected models based on evaluation may be relatively better in predicting rainfall in future period.

4 Conclusions

The coarser resolution of GCMs in CMIP5 does not provide much scope for studying the climate change assessment over the regional scale, which has varying orography, terrains, and climatic conditions. To fulfill this gap, high-resolution NEX-GDDP data may provide information at the regional level. Further, they are evaluated and assessed their performance in capturing the observed ISMR over individual homogenous monsoon regions of India. For the purpose, the observational rainfall data of APHRODITE and simulated rainfall in five models of NEX-GDDP are considered. The individual models are assessed over individual HMRI and validated against the observation by applying GPC, daily climatology, annual cycle, distribution in the box plot, the Taylor statistics, and PDF. In capturing the spatial pattern of ISMR over individual HMRI, the models in NEX-GDDP show much improved accuracy. The considered models widely agree with observation; however, over a few regions of HMRI, a mixed response is noticed. It is very crucial to find that, over the region of NEI, the model CanESM does perform well. Over the region CNI, the model MPI-ESM-LR does perform better than other models. Similarly, over the regions of PI, NWI, and WCI, models CanESM and NorESM have relatively better representation in capturing observed rainfall pattern. The relative performance of model in predicting the JJAS rainfall over the individual monsoon regions of India is summarized and shown in Table 3. Overall predictions by the model ACCESS are relatively weak. The lesser percentage bias and high GPC in the simulation of NEX-GDDP shows relatively better reliability of model for impact studies and may provide reliable projections in the near and far future time periods in compare to coarse resolution GCMs.

Acknowledgments Climate scenarios used were from the NEX-GDDP dataset, prepared by the Climate Analytics Group and NASA Ames Research Center using the NASA Earth Exchange, and distributed by the NASA Center for Climate Simulation (NCCS).

References

Bao Y, Wen X (2017) Projection of China's near- and long-term climate in a new high-resolution daily downscaled dataset NEX-GDDP. J Meteorol Res 31:236–249. https://doi.org/10.1007/s13351-017-6106-6

Bokhari SAA, Ahmad B, Ali J, Ahmad S, Mushtaq H, Rasul G (2018) Future climate change projections of the Kabul River basin using a multi-model ensemble of high-resolution statistically downscaled data. Earth Syst Environ 2:477–497. https://doi.org/10.1007/s41748-018-0061-y

Chen H-P, Sun J-Q, Li H-X (2017) Future changes in precipitation extremes over China using the NEX-GDDP high-resolution daily downscaled data-set. Atmos Ocean Sci Lett 10:403–410. https://doi.org/10.1080/16742834.2017.1367625

Christensen JH, Christensen OB (2007) A summary of the PRUDENCE model projections of changes in European climate by the end of this century. Clim Chang 81:7–30

Christensen JH, Boberg F, Christensen OB, Lucas-Picher P (2008) On the need for bias correction of regional climate change projections of temperature and precipitation. Geophys Res Lett 35. https://doi.org/10.1029/2008GL035694

Durai VR, Bhardwaj R (2014) Forecasting quantitative rainfall over India using multi-model ensemble technique. Meteorog Atmos Phys 126: 31–48. https://doi.org/10.1007/s00703-014-0334-4

Ekström M, Grose MR, Whetton PH (2015) An appraisal of downscaling methods used in climate change research. Wiley Interdiscip Rev Clim Chang 6:301–319

Errasti I, Ezcurra A, Sáenz J, Ibarra-Berastegi G (2011) Validation of IPCC AR4 models over the Iberian Peninsula. Theor Appl Climatol 103:61–79. https://doi.org/10.1007/s00704-010-0282-y

Fowler HJ, Blenkinsop S, Tebaldi C (2007) Linking climate change modelling to impacts studies: recent advances in downscaling techniques for hydrological modelling. Int J Climatol 27:1547–1578

Ghosh S, Vittal H, Sharma T, Karmakar S, Kasiviswanathan KS, Dhanesh Y, Sudheer KP, Gunthe SS (2016) Indian summer monsoon rainfall: implications of contrasting trends in the spatial variability of means and extremes. PLoS One 11:e0158670. https://doi.org/10.1371/journal.pone.0158670

Giorgi F (1990) Simulation of regional climate using a limited area model nested in a general circulation model. J Clim 3:941–963

Gregory S (1989) Macro-regional definition and characteristics of Indian summer monsoon rainfall, 1871–1985. Int J Climatol 9:465–483

Guhathakurta P, Rajeevan M (2008) Trends in the rainfall pattern over India. Int J Climatol 28:1453–1469

Hashmi MZ, Shamseldin AY, Melville BW (2011) Comparison of SDSM and LARS-WG for simulation and downscaling of extreme precipitation events in a watershed. Stoch Env Res Risk A 25:475–484

Huang J, Zhang J, Zhang Z et al (2011) Estimation of future precipitation change in the Yangtze River basin by using statistical downscaling method. Stoch Env Res Risk A 25:781–792

Mahmood R, Babel MS (2013) Evaluation of SDSM developed by annual and monthly sub-models for downscaling temperature and precipitation in the Jhelum basin, Pakistan and India. Theor Appl Climatol 113:27–44

Mandal V, De UK, Basu BK (2006) Verification of NCMRWF temperature output with observed data over West Bengal region during 2000-2002 monsoon period

Maraun D, Wetterhall F, Ireson AM et al (2010) Precipitation downscaling under climate change: recent developments to bridge the gap between dynamical models and the end user. Rev Geophys 48

Maurer EP, Hidalgo HG (2008) Utility of daily vs. monthly large-scale climate data: an intercomparison of two statistical downscaling methods

McSweeney CF, Jones RG, Lee RW, Rowell DP (2015) Selecting CMIP5 GCMs for downscaling over multiple regions. Clim Dyn 44:3237–3260. https://doi.org/10.1007/s00382-014-2418-8

Mearns LO, Bogardi I, Giorgi F et al (1999) Comparison of climate change scenarios generated from regional climate model experiments and statistical downscaling. J Geophys Res Atmos 104: 6603–6621

Meher JK, Das L, Akhter J et al (2017) Performance of CMIP3 and CMIP5 GCMs to simulate observed rainfall characteristics over the Western Himalayan region. J Clim 30:7777–7799

Parthasarathy B (1984) Interannual and long-term variability of Indian summer monsoon rainfall. Proc Indian Acad Sci Planet Sci 93:371–385

Parthasarathy B, Kumar KR, Munot AA (1993) Homogeneous Indian monsoon rainfall - variability and prediction. Proc Indian Acad Sci Planet Sci 102:121–155

Pattanaik DR, Kumar A (2010) Prediction of summer monsoon rainfall over India using the NCEP climate forecast system. Clim Dyn 34: 557–572. https://doi.org/10.1007/s00382-009-0648-y

Pepler AS, Alexander LV, Evans JP, Sherwood SC (2016) Zonal winds and southeast Australian rainfall in global and regional climate models. Clim Dyn 46:123–133. https://doi.org/10.1007/s00382-015-2573-6

Raghavan SV, Hur J, Liong SY (2018) Evaluations of NASA NEX-GDDP data over Southeast Asia: present and future climates. Clim Chang 148:503–518. https://doi.org/10.1007/s10584-018-2213-3

Rajeevan M, Bhate J, Kale JD, Lal B (2006) High resolution daily gridded rainfall data for the Indian region: analysis of break and active monsoon spells. Curr Sci 91:296–306

Rana A, Uvo CB, Bengtsson L, Sarthi PP (2012) Trend analysis for rainfall in Delhi and Mumbai, India. Clim Dyn 38:45–56. https://doi.org/10.1007/s00382-011-1083-4

Reichler T, Kim J (2008) How well do coupled models simulate today's climate? Bull Am Meteorol Soc 89:303–311. https://doi.org/10.1175/BAMS-89-3-303

Rivington M, Miller D, Matthews KB et al (2008) Downscaling regional climate model estimates of daily precipitation, temperature and solar radiation data. Clim Res 35:181–202

Sagar SK, Mrudula G, Kumari KV, Rao SVB (2017) Verification of Varsha rainfall forecasts for summer monsoon seasons of 2009 and 2010. Int J Cur Res Rev| Vol 9:24

Saha A, Ghosh S, Sahana AS, Rao EP (2014) Failure of CMIP5 climate models in simulating post-1950 decreasing trend of Indian monsoon. Geophys Res Lett 41:7323–7330. https://doi.org/10.1002/2014GL061573

Sahany S, Mishra SK, Salunke P (2019) Historical simulations and climate change projections over India by NCAR CCSM4: CMIP5 vs. NEX-GDDP. Theor Appl Climatol 135:1423–1433

Saini R, Wang G, Yu M, Kim J (2015) Comparison of RCM and GCM projections of boreal summer precipitation over Africa. J Geophys Res Atmos 120:3679–3699

Sarthi PP, Ghosh S, Kumar P (2015) Possible future projection of Indian summer monsoon rainfall (ISMR) with the evaluation of model performance in coupled model inter-comparison project phase 5 (CMIP5). Glob Planet Chang 129:92–106

Sarthi PP, Kumar P, Ghosh S (2016) Possible future rainfall over Gangetic Plains (GP), India, in multi-model simulations of CMIP3 and CMIP5. Theor Appl Climatol 124:691–701

Shukla J (1987) Interannual variability of monsoons. Monsoons:399–464

Sinha A, Cannariato KG, Stott LD et al (2007) A 900-year (600 to 1500 A.D.) record of the Indian summer monsoon precipitation from the core monsoon zone of India. Geophys Res Lett 34:1–5. https://doi.org/10.1029/2007GL030431

Solomon S, Qin D, Manning M et al (2007) Climate change 2007-the physical science basis: working group I contribution to the fourth assessment report of the IPCC. Cambridge university press

Sonali P, Kumar DN, Nanjundiah RS (2017) Intercomparison of CMIP5 and CMIP3 simulations of the 20th century maximum and minimum temperatures over India and detection of climatic trends. 465–489. https://doi.org/10.1007/s00704-015-1716-3

Sun J, Chen H (2012) A statistical downscaling scheme to improve global precipitation forecasting. Meteorog Atmos Phys 117:87–102. https://doi.org/10.1007/s00703-012-0195-7

Sunyer MA, Madsen H, Ang PH (2012) A comparison of different regional climate models and statistical downscaling methods for extreme rainfall estimation under climate change. Atmos Res 103: 119–128

Taylor KE (2001) Summarizing multiple aspects of model performance in a single diagram. J Geophys Res Atmos 106:7183–7192

Taylor KE, Stouffer RJ, Meehl GA (2012) An overview of CMIP5 and the experiment design. Bull Am Meteorol Soc 93:485–498. https://doi.org/10.1175/BAMS-D-11-00094.1

Thrasher B, Maurer EP, Duffy PB, McKellar C (2012a) Bias correcting climate model simulated daily temperature extremes with quantile mapping

Thrasher B, Maurer EP, McKellar C, Duffy PB (2012b) Technical note: bias correcting climate model simulated daily temperature extremes with quantile mapping. Hydrol Earth Syst Sci 16:3309–3314. https://doi.org/10.5194/hess-16-3309-2012

Thrasher B, Xiong J, Wang W et al (2013) Downscaled climate projections suitable for resource management. EOS Trans Am Geophys Union 94:321–323

Trzaska S, Schnarr E (2014) A review of downscaling methods for climate change projections. United States Agency Int Dev by Tetra Tech ARD 1–42

Turner AG, Annamalai H (2012) Climate change and the South Asian summer monsoon. Nat Clim Chang 2:587–595. https://doi.org/10.1038/nclimate1495

Walker GT (1925) Correlation in seasonal variations of weather—a further study of world weather. Mon Weather Rev 53:252–254

Wilby RL, Wigley TML (1998) Downscaling general circulation model output: a review of methods and limitations. Prog Phys Geogr 21: 530–548

Wilby RL, Wigley TML, Conway D, et al (1998) Statistical downscaling of general circulation model output: A comparison of methods. Water Resour Res 34:2995–3008. https://doi.org/10.1029/98WR02577

Wilby RL, Dawson CW, Barrow EM (2002) SDSM — a decision support tool for the assessment of regional climate change impacts. Environ Model Softw 17:145–157. https://doi.org/10.1016/S1364-8152(01)00060-3

Wood AW, Maurer EP, Kumar A, Lettenmaier DP (2002) Long-range experimental hydrologic forecasting for the eastern United States. J

Geophys Res D Atmos 107:1–15. https://doi.org/10.1029/2001JD000659
Wood AW, Leung LR, Sridhar V, Lettenmaier DP (2004) Hydrologic implications of dynamical and statistical approaches to downscaling climate model outputs. Clim Chang 62:189–216
Xie SP, Xu H, Saji NH et al (2006) Role of narrow mountains in large-scale organization of Asian monsoon convection. J Clim 19:3420–3429. https://doi.org/10.1175/JCLI3777.1
Yatagai A, Kamiguchi K, Arakawa O et al (2012) Aphrodite constructing a long-term daily gridded precipitation dataset for Asia based on a dense network of rain gauges. Bull Am Meteorol Soc 93:1401–1415. https://doi.org/10.1175/BAMS-D-11-00122.1
Zamani R, Berndtsson R (2018) Evaluation of CMIP5 models for west and Southwest Iran using TOPSIS-based method. Theor Appl Climatol 137:533–543. https://doi.org/10.1007/s00704-018-2616-0